Spatial Distribution of Grassland Fires at the Regional Scale Based on the MODIS Active Fire Products

International Journal of WILDLAND FIRE

Spatial Distribution of Grassland Fires at the Regional Scale Based on the MODIS Active Fire Products

Journal:	*International Journal of Wildland Fire*
Manuscript ID	WF16026.R2
Manuscript Type:	Research Paper
Date Submitted by the Author:	24-Dec-2016
Complete List of Authors:	Zhang, Zhengxiang Feng, Zhiqiang Zhang, Hongyan Zhao, Jianjun Yu, Shan Du, Wala
Keyword:	Risk, Fire history, Fire regimes

Spatial Distribution of Grassland Fires at the Regional Scale Based on the MODIS Active Fire Products

Zhengxiang Zhang[A], *Zhiqiang Feng*[B], *Hongyan Zhang*[A], *Jianjun Zhao*[A], *Shan Yu*[C], *Wala Du*[D,E]

[A]Provincial Laboratory of Resources and Environmental Research for North-east China, North-east Normal University, Changchun 130024, China

[B]School of Geosciences, University of Edinburgh, Edinburgh, EH8 9XP, Scotland, UK

[C]Inner Mongolia Autonomous Region Key Laboratory of Remote Sensing & Geography Information System, Inner Mongolia Huhhot 010022, China

[D]Ecological and Agricultural Meteorology Centre of Inner Mongolia Autonomous Region, Inner Mongolia Huhhot 010051, China

[E]Corresponding author: dwlrsgis@163.com

Abstract. Grassland fires are major disturbances to ecosystems and economies around the world. Therefore, research on the spatial patterns of grassland fires is important for understanding the dynamics of fire occurrence and providing evidence for fire prevention and management. One of the problems in grassland fire risk analysis is that historically observed fire data are generally in the point format, with imprecise positions, whereas other influencing factors are often expressed in continuous areal units. To minimize the influences of inaccurate locations and grid size, kernel density estimation, a non-parametric statistical method for estimating probability densities, can be used to produce density estimates. This method has been widely used to convert historical fire data

into continuous surfaces. In this study, kernel density estimation was applied to grassland fire events in the eastern Inner Mongolia of China, based on Moderate Resolution Imaging Spectroradiometer (MODIS) Terra and Aqua daily active fire data from 2001 to 2014. The bandwidth choice was based on the mean random distance method. Annual and seasonal kernel density maps were produced, showing that the spatial patterns of grassland fire events remained temporally consistent. These results were used to create grassland fire risk zones on the basis of the mean density values in the study area. Grassland fire prevention and planning may focus on high-risk areas identified using this method.

Additional Keywords: Grassland fire; MODIS; Kernel density estimation; Fire risk zone

Brief Summary: This study uses kernel density estimation to analyse the spatial pattern of grassland fires based on the MODIS active fire product and define grassland fire risk zones. The results show that the kernel density estimation method can be applied to analyse the spatial distribution of grassland fires.

Introduction

As one of the most important landscapes, grassland areas can be found on all continents of the world except Antarctica (Loveland et al., 2000). Fire is very common in these grass-dominated regions and grassland fires are one of the most important disturbance types in natural ecosystems (Ojima et al., 1994; Noy-Meir, 1995).

These fires are of global significance and affect the global ecosystem because the burning biomass

constitutes one of the largest sources of global greenhouse gas emissions (Hao and Liu, 1994; Oom and Pereira, 2013). Grassland fires are also harmful for agricultural and livestock production. Annual fires may result in increased soil erosion, soil degradation, loss of life and property, diminished grass resources, and reduced biodiversity (Chuvieco et al., 2010).

In the North American Great Plains and desert grasslands of southwestern North America, grassland fires mainly occur in spring and early summer, prior to the summer rainy season (Gosz et al., 1995; Gosz and Gosz, 1996; Engle and Bidwell, 2001). In the arid and semi-arid grasslands of South America, most grassland fires are repeatedly ignited to suppress undesirable woody vegetation (Bóo et al., 1996; Bóo et al., 1997; Guevara et al., 1999; Martinez Carretero, 1995). In Africa, widespread fires frequently burn the savanna each year, and most fires occur in dry seasons (June–August) (Danthu et al., 2003; Laris, 2002; Mbow et al., 2000; Reid et al., 2000; Sheuyange et al., 2005; Snyman, 2004). In Australia, vast tracts of savanna are burnt annually in the dry season (May–November) under relatively severe climatic conditions (Edwards et al., 2001; Gill et al., 1996). As a major part of Asian grasslands, arid and semi-arid grasslands cover Mongolia and the Inner Mongolia of China. Annual fires are also frequent in these areas. The cycle of fire occurrence is about 3–6 years, and over 90% occur in spring and autumn (Liu et al., 1999; Zhou, 1995).

In order to estimate fire risk, fire managers and scientists have studied the phenomenon in terms of frequency, severity, size, probability, spatial pattern and distribution (Amatulli et al., 2007). Fire risk assessment would help the managers in making fire prevention and management plans according to spatial and temporal patterns in the high risk zones. Mapping fire risk zones using spatial and temporal models of wildland fire history or fire occurrence is essential from ecological,

social and economic perspectives (Pleniou et al., 2013).

To assess fire risk, data on the historical fire occurrence and environmental factors must be available to fire managers or scientists. However, it is often the case that the historical fire records do not contain the proper information regarding fire events, such as the mean or approximate geographical location, size, perimeter and severity. Although a fire event is often treated as a point in x- and y-coordinates, point recognition process of events would lead to serious positional inaccuracies because the exact location of ignition point is usually unknown (Amatulli et al., 2007; Koutsias et al., 2004; Kuter et al., 2011).Human activities are closely associated with fire occurrences. Data on human and economic factors are largely sourced from administrative records at different spatial scales. Combining these inaccurate fire records and administrative records regarding influencing factors may result in substantial errors when we examine the spatial patterns of fire and their influencing factors. In other words, risk assessment that integrates firs evens and human factors would benefit from the continuous form of fire events because of the ease of integration with data on human activities and reduced error propagation in the process (Syphard et al., 2007; Martinez et al., 2009; Martinez-Fernandez et al., 2013). Therefore, a reliable method is necessary to convert the fire occurrence point data into a continuous surface representing the fire occurrence density and to carry out the fire risk zoning exercise (Koutsias et al., 2004).

There are several interpolation techniques used to convert data from fire points to continuous surfaces. As a commonly preferred method, Kernel density estimation (KDE) produces a surface that is a nonparametric estimate of the underlying unknown intensity function (Waller, 2004). This method has been widely used to convert historical forest fire occurrence data into continuous fire occurrence density surfaces, to identify the spatial patterns of fire occurrence at the regional or

local scales and to assess the forest fire risk associated with the influencing factors (Amatulli et al., 2007; Koutsias et al., 2004; Kuter et al., 2011). These analyses suggest that this type of spatial pattern information is very useful for predicting and managing forest fires.

Most grassland involves annual vegetation, and these grass fuels can ignite every year in suitable environments. In comparison, grassland fires release energy at a rate lower than that of forest fires (Mell et al., 2005). Forest fires have very large ecological impacts on all of the vegetation strata in a forest. However, because grassland fuels are more flammable and have lower moisture contents, grassland fires occur more easily and propagate more quickly. Therefore, grassland fires may represent high-risk situations, especially during suppression operations (Alexander and Fogarty, 2002; Linn et al., 2002). To understand and manage grassland fires, it is critical to analyze the distributions of grassland fires.

The main purpose of this study is to reveal the spatial patterns of grassland fire events in the eastern Inner Mongolia of China, which has suffered from high incidence of grassland fire , using KDE methods with MODIS fire active products (from 2001 to 2014) and to demonstrate that such a technique can be applied in grassland fire analysis. Seasonal and annual KDE maps were produced to disclose the time dimension of fire regimes. . The final density map of grassland fire occurrence zones shows the mean density in the study area and has potential to help improve preventative management strategies of grassland fires.

Materials and Methods

Study Area

The study area is located in the eastern Inner Mongolia Autonomous Region of China, between

41.26-53.23°N and 115.22-126.06°E (Figure 1). It is approximately 1,333 km long and 743 km wide, covering a total area of 454,204 km^2. The climate in the study area is a typical temperate continental monsoon, with low, irregular rainfall and extreme changes in temperature between summer and winter. The annual mean air temperature and precipitation are approximately -2.3°C and 320 mm respectively (Zhang et al., 2013). The vegetation in the eastern Inner Mongolia grassland region is made up of diverse plant communities, which are dominated by *Stipa baicalensis, Filifolium sibiricum* and *Leymus chinensis*. The elevation ranges between 200 and 1500 m. The central region is dominated by the Daxing'An Mountains, stretching from the centre of the region towards the east and west. The elevation gradually decreases, and topography gradually becomes flatter. There are 36 counties and approximately 5000 villages and towns scatter across the study area. Paved roads, dirt roads, and railroads are common in the region. They are distributed throughout the area, with an average density of approximately 67.64 km/km^2. The activities of the inhabitants often lead to accidental fires. The annual frequency of fires in the region is high with approximately 600 wildfires every year, which is why it was chosen as the study area (Fu et al., 2001).

Data

In the study area, traditional methods were used to collect information on fire events via the officers of local fire protection departments. The MODIS Active Fire Data contain daily fire pixel locations that are most appropriate for analysing the spatial and temporal distributions of events. The MODIS Terra and Aqua daily active fire product data (MOD14A1 and MYD14A1) are available in our study region. The fire product data set from 2001 to 2014 was downloaded from

the Land Processes Distributed Active Archive Centre (LP-DAAC) using a web-based interface known as Reverb, which is a replacement for the Warehouse Inventory Search Tool (https://reverb.echo.nasa.gov/). This fire product is based on 1 km pixels, in which burning was detected at the times of Terra and Aqua satellite overpassing under relatively cloud-free conditions. A contextual algorithm that detects the strong emission of mid-infrared radiation from fires is used based on brightness temperatures derived from the 4 and 11 μm channels, enhancing the sensitivity of smaller, cooler fires and minimising the detection of false positives (Giglio et al., 2003; Morisette et al., 2005; Giglio et al., 2006; de Klerk et al., 2008; Hawbaker et al., 2008).

The fire mask is the principle component of the Level 2 MODIS fire product and is stored as an 8-bit unsigned integer Scientific Data Set (SDS). In it, individual 1 km pixels are assigned to one of nine classes (Giglio, 2013). These classes are listed in Table 1. It was found that classes eight and nine of the fire mask pixel are suitable for the study area (He et al., 2013). The pixels with values of eight and nine were extracted from the MOD14A1 and the downloaded rasters were converted into the vector format as active fire points.

A land use and land cover data set of the study area was provided by the Data Centre for Resources and Environmental Sciences, Chinese Academy of Sciences (RESDC) (http://www.resdc.cn). These data were interpreted from Landsat TM/ETM from 2010 at the scale of 1:100,000. The grasslands in the study area were derived from the land use data set. Then, the active fire data set was overlaid by grasslands to erase the non-grassland fire events. The occurrence counts and coordinates were saved in an attribute table. Then, all the active grassland fires were compounded into one layer.

The standard map of the study area in the digital format and grassland fire data obtained from

MODIS were all set to the scale of 1:100,000 and the Transverse Mercator projection with D_WGS_1984 datum.

KDE Methods

The implementation of kernel density estimation is based on the estimation of the density at each intersection of a grid of quadrants superimposed on the data after assigning a probability density to each event (Levine, 2000; Seaman and Powell, 1996). The estimated density results from the sum of the densities of all the kernels overlapping at each grid cell (Worton, 1989; Tufto et al., 1996).

Kernel density estimation, a non-parametric statistical method for estimating probability densities, has been widely used for home range estimation in wildlife ecology and for forest fire risk assessment (Amatulli et al., 2007; Boer et al., 2009; Koutsias et al., 2014; Kuter et al., 2011).

The bivariate kernel density estimator was mathematically defined by Silverman as follows (1998):

$$\hat{f}(x) = \frac{1}{nh^2} \sum_{i=1}^{n} K \frac{1}{h}(x - X_i) \quad (1)$$

where n is the number of points, h is the smoothing parameter or the bandwidth, K is a kernel density function, x is a vector of coordinates that represent the location where the function is estimated, and X_i represents vectors of coordinates that define each observation.

The kernel function can be selected from a variety of functions (De La Riva et al., 2004). In this study, the Epanechnikov kernel function was selected, which is the default in ArcGIS. This function is defined by Silverman as follows (1998).

176
$$K_e(x)=\begin{cases}\frac{1}{2}C_d^{-1}(d+2)(1-x^Tx) & if: x^Tx<1\\ 0 & otherwise\end{cases} \quad (2)$$

177 The bandwidth influences the smoothness of the density function by controlling the size of the
178 kernel and the interpolation results. A narrow bandwidth generates a finer mesh density, and a
179 larger bandwidth produces a smoother density distribution (Amatulli et al., 2007). Several
180 methods can be used to find the appropriate size of the bandwidth (Worton, 1989; De La Riva et
181 al., 2004).

182 To avoid the different effects of the active fire points over the areas with different degrees of
183 concentration, the mean random distance (RDmean) of an equal number of randomly distributed
184 points over an area should be considered (Koutsias et al., 2004). RDmean refers to the distribution
185 of the total number of points in a specific area. If the number of points is large, a small bandwidth
186 would be more suitable, avoiding loss of variability in the estimates. For a small number of points,
187 a large bandwidth should be adopted to avoid density estimations associated with nothing more
188 than random variability (Koutsias et al., 2004). In the present study, the RDmean method was
189 selected for the kernel bandwidth calculation. It can be based on a local or global approach. In the
190 local approach, the mean compartment area size and mean number of active fire points per
191 compartment are taken into account, whereas total size of the study area and total number of
192 active fire points are considered in the global approach. The RDmean function is defined as
193 follows (De La Riva et al., 2004):

194
$$RDmean=\frac{1}{2}\sqrt{\frac{A}{N}} \quad (3)$$

195 where A is mean polygon size and N is mean number of active fire points inside a compartment in
196 the local approach. In the global approach, A is the total area of the study area and N is the total

number of points in the study area.

The double of the RDmean value was recommended as the bandwidth value in previous studies (Koutsias et al., 2004; De La Riva et al., 2004). Therefore, the KDE maps of active grassland fires were generated seasonally and in three periods (2001-2005, 2006-2010, 2011-2014) using values of twice the RDmean.

Accuracy assessment

The Monthly Tiled 500 m Burned Area Product (MCD45A1) in the study area from 2001 to 2014 was downloaded from the website (https://reverb.echo.nasa.gov/). The pixels with values corresponding to the approximate Julian day of the burning were considered burned areas, and all other codes were indicated as non-burned (Boschetti et al., 2013). The pixel values were set to one for burned cells and zero for non-burned cells. The monthly burned area data sets were masked by grassland data. According to the Julian day value, the masked data sets were overlaid using map algebra and compiled into three periods (2001-2005, 2006-2010, and 2011-2014) and seasonal data sets (spring (Julian day 334-60), summer (Julian day 61-151), autumn (Julian day 152-242) and winter (Julian day 243-333)). Then, the pixel values reflected the burn times of each grid in corresponding periods.

To characterize the sensitivity of the KDE results for grassland fires, the pixels in burned areas and the same number of pixels from non-burned areas in each period were randomly selected. The corresponding pixels of KDE results were also selected. All values of selected pixels were inputted into SPSS software (ver. 14), and Pearson correlation coefficients in each period were provided to assess the sensitivity of the KDE application to grassland fires.

Mapping of grassland fire risk zones

In the study area, the KDE mapping of active grassland fires was carried out to analyse the characteristics of the fire distribution. To assess the differences in fire regimes between counties for supporting decision making and fire prevention policies, each county in the study area was considered a compartment, and the mean density value in each compartment was generated based on the kernel density surfaces. Furthermore, fire risk zones were generated with five categories (very high, high, moderate, low and very low) using the mean density value in each compartment based on the criterion of the "quantile" method. ArcGIS (ver. 10.2) was used to implement the KDE method and produce maps.

Results

The grassland fire events in the entire study area are shown in Figure 2, and the total number of grassland fires was 6020 over the 14 years between 2001 and 2014 (Table 2). The years with the largest number of events were 2003 and 2014. Years 2004 and 2001 witnessed the lowest number of fires. Annually, the peak months were April, March, September and May, and the months with the fewest fire events were January, December and July. Figure 3 shows the monthly time series of grassland fire events. The time series reveals seasonal patterns, with a large number of events between March and May and a peak in April. A secondary peak occurs between August and October, with a peak in September. The seasonal characteristics of grassland fires are obvious. The probabilities of grassland fire occurrence in the study area from high to low are spring, autumn, summer and winter.

The double of the RDmean value was used as the bandwidth value in the KDE calculations. The parameters used in bandwidth calculations and bandwidth values are given in Table 3. For the mean random distance approach, the bandwidth was calculated using local and global mean random distance calculations and both approaches yielded the same bandwidth value of 8686 m. Using the final bandwidth value, seasonal and annual KDE maps were obtained.

According to the seasonal KDE maps, grassland fire points show different spatial and temporal clustering patterns (Figure 4). In the spring, the spatial distribution of grassland fires is clustered significantly compared to those in other seasons. The largest proportion of grassland fires occurred in spring, with a percentage of 59.53%, out of all the active fire events. In descending order, the other proportions are autumn (30.52%), summer (7.84%) and winter (2.11%). The largest occurrence densities of grassland fires in each season are 0.358 times/km^2, 0.248 times/km^2, 0.129 times/km^2 and 0.049 times/km^2. The high-density areas are located in the northern part of the study area, especially in the northeast part.

Three periods: 2001-2005, 2006-2010 and 2011-2014 were separately summarized and analysed. The percentages of fire events in the three periods are respectively 35.3%, 31.76% and 32.71%. There are no significant differences between the numbers of grassland fire events. KDE maps generated for these periods are shown in Figure 5. It can be seen that there is a gradual decrease in active fire events after 2005, but the trend reversed after 2010. The spatial distributions of grassland fire events are similar in these three periods. Grassland fire events were dense in the north and the northeast parts of the study area. In the southern part, the density was significantly lower, with the density in 2006-2010 being the lowest.

Table 4 shows the results of the statistical comparison between the burned and non-burned pixel

values and the corresponding values of grassland fire KDE maps in each period. Based on a Pearson Correlation test, the results are statistically significant. It shows that the burned areas have significant positive correlations with the kernel density surfaces. The results confirm the validity and sensitivity of the KDE method for application in grassland fire studies.

The kernel density surface was generated over the whole period (2001-2014), and each compartment in the study area was reclassified into five classes according to the mean density value to create zones of grassland fire occurrence (Figure 6). The reclassification of the mean density value was again based on the "quantile" method in each zone. From high to low, each zone was labelled as very high, high, moderate, low and very low. The percentage of the total study area covered by each fire occurrence risk zone is as follows: very high, 31.66%; high, 15.07%; moderate, 13.47%; low, 23.2%; and very low, 16.60%. Notably, over 46% of the east Inner Mongolia grassland falls within a high fire risk zone.

Conclusions

Fire management departments make operational strategies for supressing, preventing and forecasting grassland fires. Currently, the northwest part of the study area, the Hulunbeir Grassland, is the top priority in the strategy of preventing grassland fires because it is a large and continuous grassland. The administrative management in this region focuses on preventing fire occurrence and reducing losses associated with grassland fires (Liu, 2016). According to our results (Figures 4 and 5), the Hulunbeir grassland has nearly the lowest fire density. However, the high fire risk zones with small and fragmented grassland patches are not areas where the management activities focus on because the fires would result in less human and economic losses.

To analyse the grassland fire risk and take effective measures, fire risk zone mapping with the KDM method might provide a strategic operational advantage for proper development of decision support systems.

Although the active fire data of MODIS MOD14A1 and MYD14A1 products contain x- and y-coordinates of fire events, they are in the point format and thus different from continuous areal data that express anthropogenic, topographic and climatic conditions. As a nonparametric method for obtaining continuous surfaces from point observations, KDE has been widely used to convert historical fire data into forest fire density maps.

In this study, grassland fire risk zones were produced using historical grassland fire occurrence data from MODIS from 2001 to 2014 based on the KDE method. When preparing KDE maps of grassland fires, the mean random distance method for the calculation of bandwidth was used based on the mean compartment size and mean number of active fire events per polygon, as well as the global area and total active number of fire events. The seasonal and yearly KDE maps present the same spatial distribution patterns. In the spring and autumn seasons and in the north and northeast parts of the study area where the fire risk is high, prevention and safety measures should be strengthened.

This paper develops a method of mapping fire risk based on historical data. It demonstrates that grassland fire density mapping by KDE together with the MODIS active fire products has the potential to assist grassland fire management agencies in developing appropriate management strategies in areas that are more prone to fire hazard.

Acknowledgements

This study was sponsored by the National Natural Science Foundation of China (project no. 41571489, no. 41461102 and 41501449) and National Science and Technology Major Project of China (project no. 2015ZX07201-008-10)

References

Alexander ME, Fogarty LG (2002) A pocket card for predicting fire behaviour in grasslands under severe burning conditions. *Fire Technology Transfer Note* 25, 1-8.

Amatulli G, Perez-Cabello F, De la Riva J (2007) Mapping lightning/human-caused wildfires occurrence under ignition point location uncertainty. *Ecological Modeling* 200 (3-4), 321-333.

Boer MM, Sadler RJ, Wittkuhn RS, Mccaw L, Grierson PF (2009) Long term impacts of prescribed burning on regional extent and incidence of wildfires - evidence from 50 years of active fire management in SW Australian forests. *Forest Ecology and Management* 259, 132-142.

Bóo RM, Peláez DV, Bunting SC, Elía OR (1996) Mayor, M.D. Effect of fire on grasses in central semi-arid Argentina. *Journal of Arid Environments* 32, 259-269.

Bóo RM, Peláez DV, Bunting SC, Mayor MD, Elía OR (1997) Effect of fire on woody species in central semi-arid Argentina. *Journal of Arid Environments* 35, 87-94.

Boschetti L, Roy D, Hoffmann AA, Humber M (2013) MODIS Collection 5.1 Burned Area Product User's Guide, Version 3.0. University of Maryland, P 14. Available online: http://modis-fire.umd.edu/files/MODIS_Burned_Area_Collection51_User_Guide_3.0.pdf

Chuvieco E, Aguado I, Yebra M, Nieto H, Salas J, Pilar Martín M, Vilar L, Vega JM, Martín S, Ibarra P, de la Riva J, Baeza MJ, Silva FR, Machuca MAH, Zamora R (2010) Development of a frame work for fire risk assessment using remote sensing and geographic information system

technologies. *Ecological Modeling* 221, 46-58.

Danthu P, Ndongo M, Diaou M, Thiam O, Sarr A, Dedhiou B, Vall AOM (2003) Impact of bush fire on germination of some West African Acacias. *Forest Ecology and Management* 173, 1-10.

de Klerk H (2008) A pragmatic assessment of the usefulness of the MODIS (Terra and Aqua) 1-km active fire (MOD14A2 and MYD14A2) products for mapping fires in the fynbos biome. *International Journal of Wildland Fire* 17, 166-178.

De La Riva J, Pérez-Cabello F, Lana-Renault N, Koutsias N (2004) Mapping wildfire occurrence at regional scale. *Remote Sensing of Environment* 92, 363-369.

Edwards A, Hauser P, Anderson M, McCartney J, Armstrong M, Thackway R, Allan G, Hempel C, Russell-Smith J (2001) A tale of two parks: contemporary fire regimes of Litchfield and Nitmiluk National Parks, monsoonal northern Australia. *International Journal of Wildland Fire* 10, 79-89.

Engle DM, Bidwell TG (2001) Viewpoint: the response of central North American prairies to seasonal fire. *Journal of Range Management* 54, 2-10.

Fu ZQ, Yang YX, Dai EF (2001) Research on fire dynamics and fire risk climate divisions in Inner Mongolia. Journal of China Agricultural Resources and Regional Planning 22(6), 18-22.

Giglio L (2013) MODIS Collection 5 Active Fire Product User's Guide, Version 2.5. Department of Geographical Sciences, University of Maryland, p18. Available online: http://modis-fire.umd.edu/files/MODIS_Fire_Users_Guide_2.5.pdf

Giglio L, Descloitres J, Justice CO, Kaufman YJ (2003) An enhanced contextual fire detection algorithm for MODIS. *Remote Sensing of Environment* 87, 273-282.

Giglio L, van derWerf GR, Randerson JT, Collatz GJ, Kasibhatla P (2006) Global estimation of burned area using MODIS active fire observations. *Atmospheric Chemistry and Physics* 6,

957-974.

Gill AM, Moore PHR, Williams RJ (1996) Fire weather in the wet–dry tropics of the World Heritage Kakadu National Park, Australia. *Australian Journal of Ecology* 21, 302-308.

Gosz JR, Moore DI, Shore GA, Grover H,D, Rison W, Rison C (1995) Lightning estimates of precipitation location and quantity on the Sevilleta LTER, New Mexico. *Ecological Applications* 5(4), 1141-1150.

Gosz RJ, Gosz JR (1996) Species interactions on the biome transition zone in New Mexico: response of blue grama (Bouteloua gracilis) and black grama (Bouteloua eripoda) to fire and herbivory. *Journal of Arid Environments* 34(1), 101-114.

Guevara JC, Stasi CR, Wuilloud CF, Estevez OR (1999) Effects of fire on rangeland vegetation in south-western Mendoza plains (Argentina): composition, frequency, biomass, productivity and carrying capacity. *Journal of Arid Environments* 41, 27-35.

Hao WM, Liu MH (1994) Spatial and temporal distribution of tropical biomass burning. *Global Biogeochemical Cycles 8*, 495–503.

Hawbaker TJ, Radeloff VC, Syphard D, Zhu Z, Stewart S (2008) Detection rates of the MODIS active fire product in the United States. *Remote Sensing of Environment* 112, 2656-2664.

He C, Gong YX, Zhang SY, He TF, Chen F, Sun Y, Feng ZK (2013) Forest fire division by using MODIS data based on the temporal-spatial variation law. *Spectroscopy and Spectral Analysis* 33(9), 2472-2477. [in Chinese]

Koutsias N, Balatsos P, Kalabokidis K (2014) Fire occurrence zones: kernel density estimation of historical wildfire ignitions at the national level, Greece. *Journal of Maps* 10(4), 630-639.

Koutsias N, Kalabokidis KD, Allgower B (2004) Fire occurrence patterns at landscape level:

beyond positional accuracy of ignition points with kernel density estimation methods. *Natural Resource Modeling* 17(4), 359-375.

Kuter N, Yenilmez Y, Kuter S (2011) Forest fire risk mapping by Kernel density estimation. *Croatlan Journal of Forest Engineering* 32(2), 599-610.

Kuter S, Usul N, Kuter N (2011) Bandwidth determination for kernel density analysis of wildfire events at forest sub-district scale. *Ecological Modelling* 222, 3033-3040.

Laris P (2002) Burning the seasonal mosaic: preventive burning strategies in the wooded savanna of southern Mali. *Human Ecology* 30, 155-186.

Levine N (2000) CrimeStat: A Spatial Statistics Program for the Analysis of Crime Incident Locations (Version 1.1), Ned Levine and Associates, Annandale, VA and The National Institute of Justice, Washington, DC.

Linn RR, Reisner J, Colman JJ, Winterkamp J (2002) Studying wild fire behavior using FIRETEC. *International Journal of Wildland Fire* 11, 233-246.

Liu GX, Su H, Li SL (1999) The summarization on the fire accident of grassland in Inner Mongolia. *Grassland of China* 4, 76-78. [in Chinese]

Liu Y (2016) Report of monitoring grassland. *China Animal Industry* 6, 18-35. [in Chinese]

Loveland TR, Reed BC, Brown JF (2000) Development of a global land cover characteristics database and IGBP discover from 1km AVHRR data. *International Journal of Remote Sensing* 21, 1303-1330.

Martinez-Fernandez J, Chuvieco E, Koutsias N (2013) Modelling long-term fire occurrence factors in Spain by accounting for local variations with geographically weighted regression. *Natural Hazards and Earth System Sciences* 13, 311-327.

395 Martinez Carretero E (1995) Los incendios forestales en la Argentina. *Multequina* 4, 105-114.

396 Mbow C, Nielsen TT, Rasmussen K (2000) Savanna fires in east-central Senegal: distribution
397 patterns, resource management perceptions. *Human Ecology* 28, 561-583.

398 Martinez J, Vega-García C, Chuvieco E (2009) Human-caused wildfire risk rating for prevention
399 planning in Spain. *Journal of Environmental Management* 90, 1241-1252.

400 Mell W, Charney JJ, Jenkins MA, Cheney NP, Gould J (2005) Numerical simulations of grassland
401 fire behavior from the LANL-FIRETEC and NIST-WFDS models. In: Proceedings of the East
402 FIRE Conference, May11–13, Fairfax, VA, 10p.

403 Morisette JT, Giglio L, Csiszar I, Setzer A, Schroeder W, Morton D, Justice CO (2005)
404 Validation of MODIS active fire detection products derived from two algorithms. *Earth*
405 *Interactions* 9(9), 1-25.

406 Noy-Meir I (1995) Interactive effects of fire and grazing on structure and diversity of
407 Mediterranean grasslands. *Journal of Vegetation Science* 6, 701-710.

408 Ojima DS, Schimel DS, Parton WJ, Owensby CE (1994) Long- and short-term effects of fire on
409 nitrogen cycling in tallgrass prairie. *Biogeochemistry* 24, 67-84.

410 Oom D, Pereira JMC (2013) Exploratory spatial data analysis of global MODIS active fire data.
411 *International Journal of Applied Earth Observation and Geoinformation* 21, 326-340.

412 Pleniou M, Xystrakis F, Dimopoulos P, Koutsias N (2013) Maps of fire occurrence - spatially
413 explicit reconstruction of recent fire history using satellite remote sensing. *Journal of Maps* 8,
414 499-506.

415 Reid RS, Kruska RL, Muthui N, Taye A, Wotton S, Wilson CJ, Mulatu W (2000) Land-use and
416 land-cover dynamics in response to changes in climatic, biological and socio-political forces: the

417 case of southwestern Ethiopia. *Landscape Ecology* 15, 339-355.

418 Seaman ED, Powell RA (1996) An Evaluation of the Accuracy of Kernel Density Estimators for

419 Home Range Analysis. *Ecology* 77, 2075-2085.

420 Sheuyange A, Oba G, Weladji RB (2005) Effects of anthropogenic fire history on savanna

421 vegetation in northeastern Namibia. *Journal of Environmental Management* 75(3), 189-198.

422 Silverman BW (1998) Density estimation for statistics and data analysis. Chapman & Hall/CRC,

423 USA, p175.

424 Snyman HA (2004) Short-term response in productivity following an unplanned fire in a semi-arid

425 rangeland of South Africa. *Journal of Arid Environments* 56, 465-485.

426 Syphard AD, Radeloff VC, Keeley JE, Hawbaker TJ, Clayton MK, Stewart SI, Hammer RB (2007)

427 Human influence on California fire regimes. *Ecological Applications* 17(5), 1388-1402.

428 Tufto J, Andersen R, Linnell J (1996) Habitat Use and Ecological Correlates of Home Range Size

429 in a Small Cervid: The Roe Deer. *Journal of Animal Ecology* 65, 715-724.

430 Waller LA, Gotway CA (2004) Applied Spatial Statistics for Public Health Data. John Wiley &

431 Sons, Inc., Hoboken, New Jersey, USA, p494.

432 Worton BJ (1989) Kernel Methods for Estimating the Utilization Distribution in Home-Range

433 Studies. *Ecology* 70, 164-168.

434 Zhou DW (1995) Method for determining fire cycle in treeless meadow grasslands. *Acta*

435 *Ecologica Sinica* 15(1), 61-65. [in Chinese]

436

437

438

Table 1: MOD14/MYD14 fire mask pixel classes

Class	Meaning
0	Not processed (missing input data)
2	Not processed (other reason)
3	Water
4	Clouds
5	Non-fire clear land
6	Unknown
7	Low-confidence fire
8	Nominal-confidence fire
9	High-confidence fire

451

452

453 Table 2: The number of grassland fire events by year and month

Year	Month												Total	Percent
	1	2	3	4	5	6	7	8	9	10	11	12		(%)
2001	0	0	59	104	13	4	1	3	51	4	14	0	253	4.20
2002	0	18	58	21	12	13	6	41	44	28	63	0	304	5.05
2003	0	18	287	127	350	51	5	3	6	4	1	0	852	14.15
2004	0	5	10	56	6	24	14	33	10	31	7	2	198	3.29
2005	1	1	87	96	18	19	3	33	169	99	6	0	532	8.84
2006	0	1	22	118	128	10	2	6	121	16	1	1	426	7.08
2007	1	27	18	144	18	7	6	42	61	7	0	8	339	5.63
2008	0	18	279	83	21	7	1	7	29	9	22	3	479	7.96
2009	0	4	8	126	70	1	2	2	46	60	21	0	340	5.65
2010	0	3	5	62	41	14	5	12	70	100	16	0	328	5.45
2011	0	3	19	228	11	8	2	17	44	37	9	0	378	6.28
2012	0	3	79	131	43	6	2	17	28	13	12	0	334	5.55
2013	0	0	1	99	135	6	8	4	103	105	42	1	504	8.37
2014	2	6	155	221	15	9	6	10	223	88	18	0	753	12.51
Total	4	107	1,087	1,616	881	179	63	230	1,005	601	232	15	6,020	100.00
Percent (%)	0.07	1.78	18.06	26.84	14.63	2.97	1.05	3.82	16.69	9.98	3.85	0.25	100.00	

454

455

456

457 Table 3: Parameters related to bandwidth calculations

Total size of the study area, A	454,204.51 km^2
Total number of polygons	36
Total number of active fire events, N	6,020
Mean polygon size	12,616.79 km^2
Mean number of active fire events per polygon	167.22
Local RDmean	8,686.21 m
Global RDmean	8,686.15 m

458

459

460

461 Table 4: The Pearson Correlation Coefficients for the burned and non-burned area pixel values and

462 the corresponding pixel values of grassland fire KDE maps in each period

Pixel values of KDE maps		Pixel values of burned and non-burned areas
2001-2005	Pearson Correlation	.470**
	Sig. (2-tailed)	.000
	N	10,336
2006-2010	Pearson Correlation	.613**

	Sig. (2-tailed)	.000
	N	3,600
2011-2014	Pearson Correlation	.469**
	Sig. (2-tailed)	.000
	N	4,988
Spring	Pearson Correlation	.489**
	Sig. (2-tailed)	.000
	N	13,114
Summer	Pearson Correlation	.317**
	Sig. (2-tailed)	.000
	N	697
Autumn	Pearson Correlation	.433**
	Sig. (2-tailed)	.000
	N	4,192
Winter	Pearson Correlation	.539**
	Sig. (2-tailed)	.000
	N	166

**Correlation is significant at the 0.01 level (2-tailed)

468

469

470 Figure 1: The location of the study area in the east Inner Mongolia Autonomous Region of China

471 Figure 2: Distribution of grassland fire events from 2001 to 2014 observed by MODIS

472 Figure 3: Monthly time series of grassland active fire events

473 Figure 4: The KDE maps in different seasons: (a) spring, (b) summer, (c) autumn and (d) winter

474 Figure 5: The KDE maps of different periods from 2001-2005, 2006-2010 and 2011-2014

475 Figure 6: The KDE map of the whole study period (2001-2014) (a) and grassland fire risk map of

476 the study area according to the mean density value of KDE (b)

477

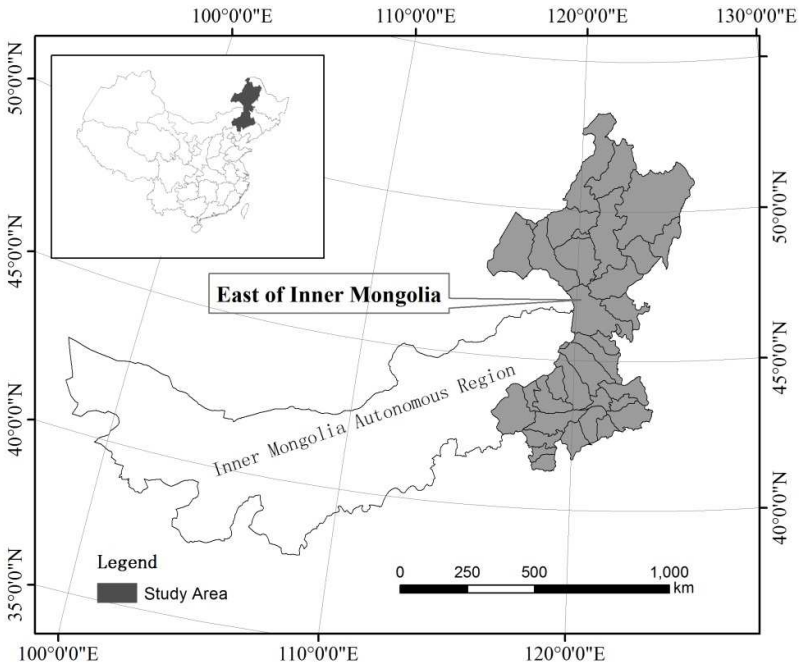

Figure 1: The location of the study area in the east Inner Mongolia Autonomous Region of China

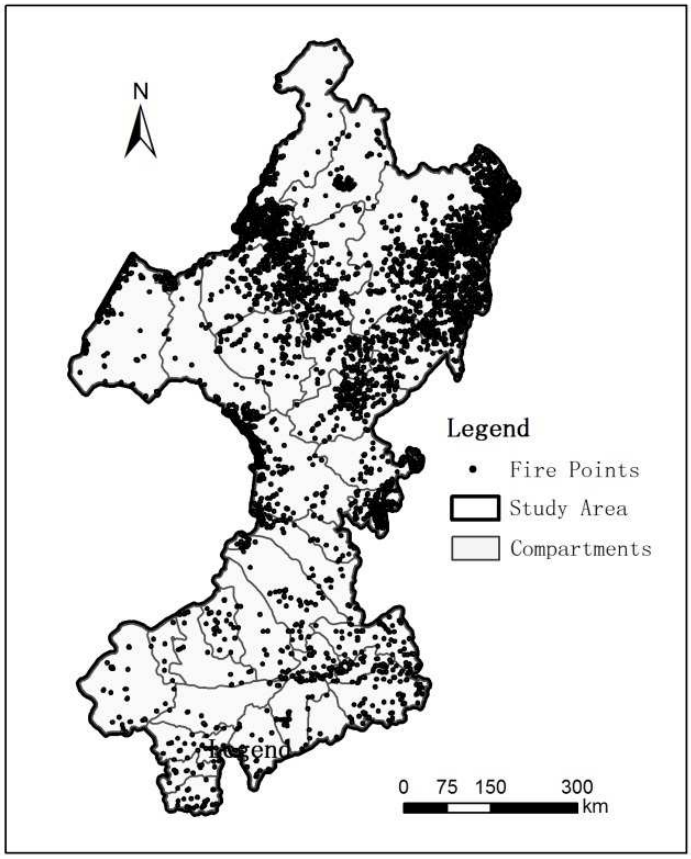

Figure 2: Distribution of grassland active fire points from 2001 to 2014 observed by MODIS

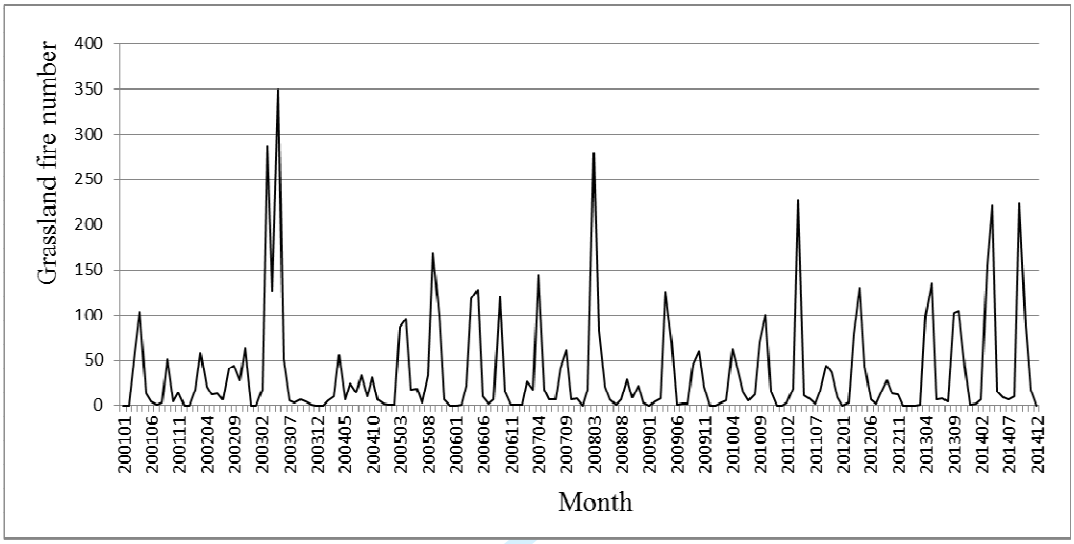

Figure 3: Monthly time series of grassland active fire events

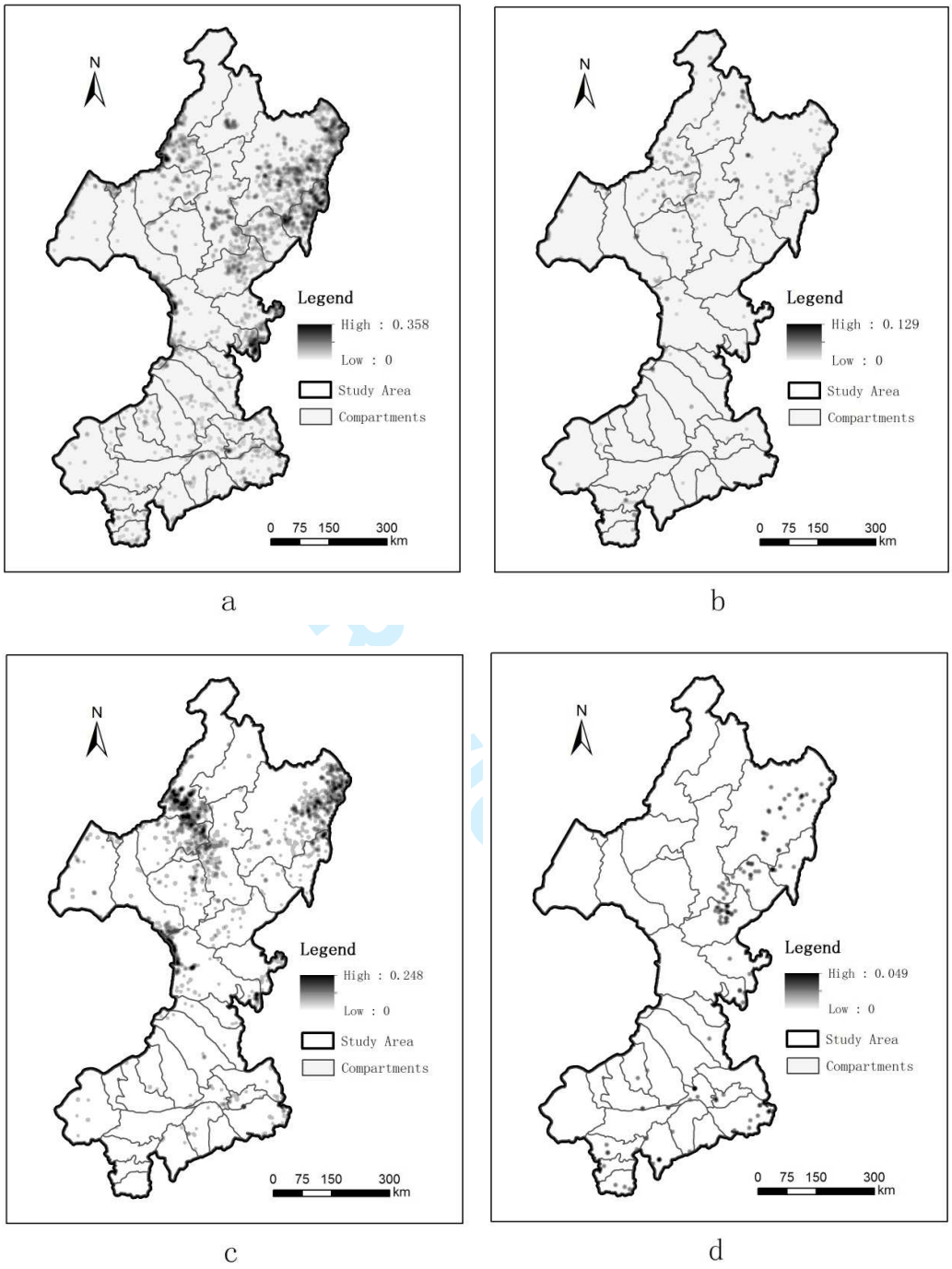

Figure 4: The KDE maps in different seasons: (a) spring, (b) summer, (c) autumn and (d) winter

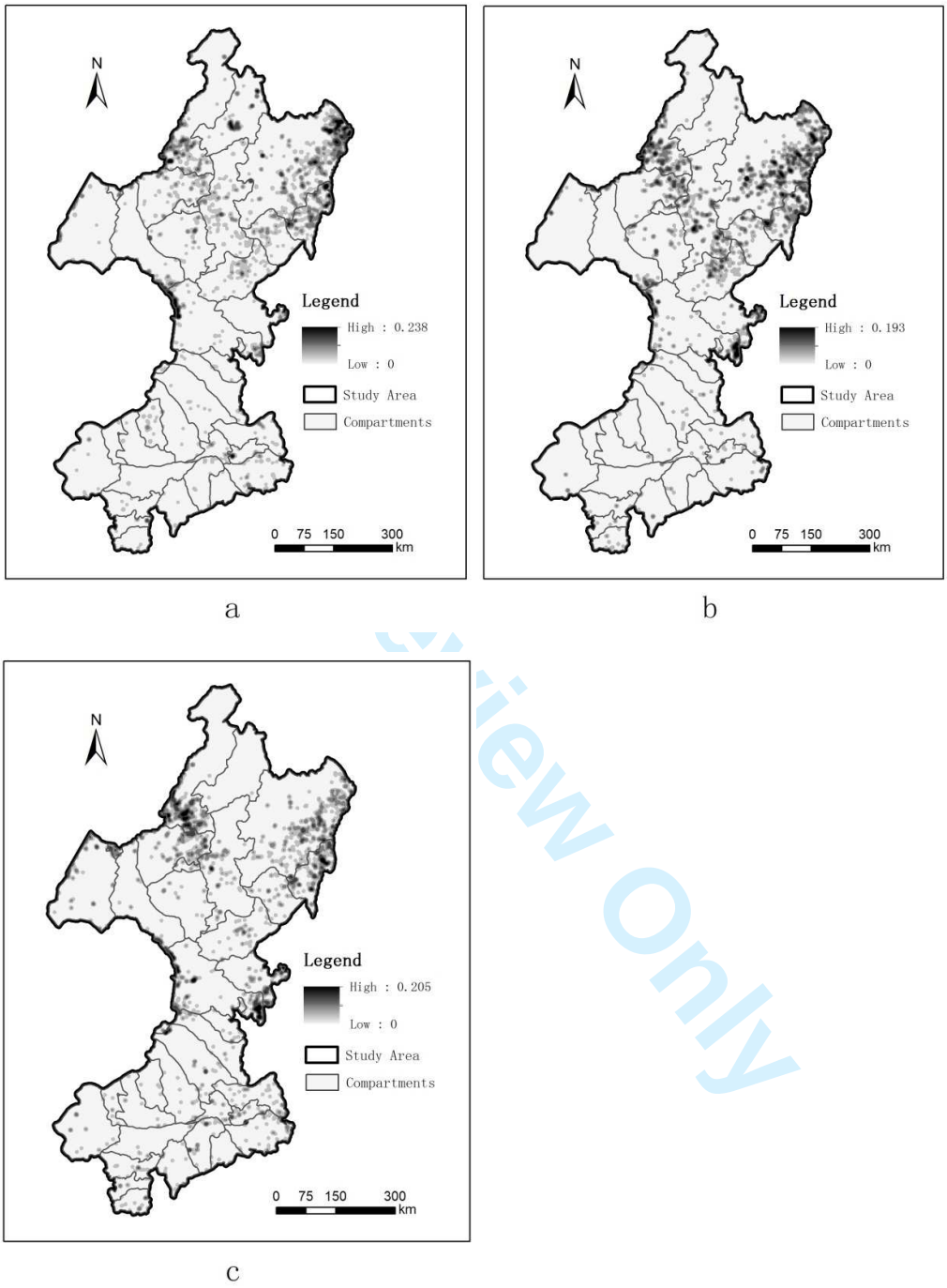

Figure 5: The KDE maps of different periods from 2001-2005, 2006-2010 and 2011-2014

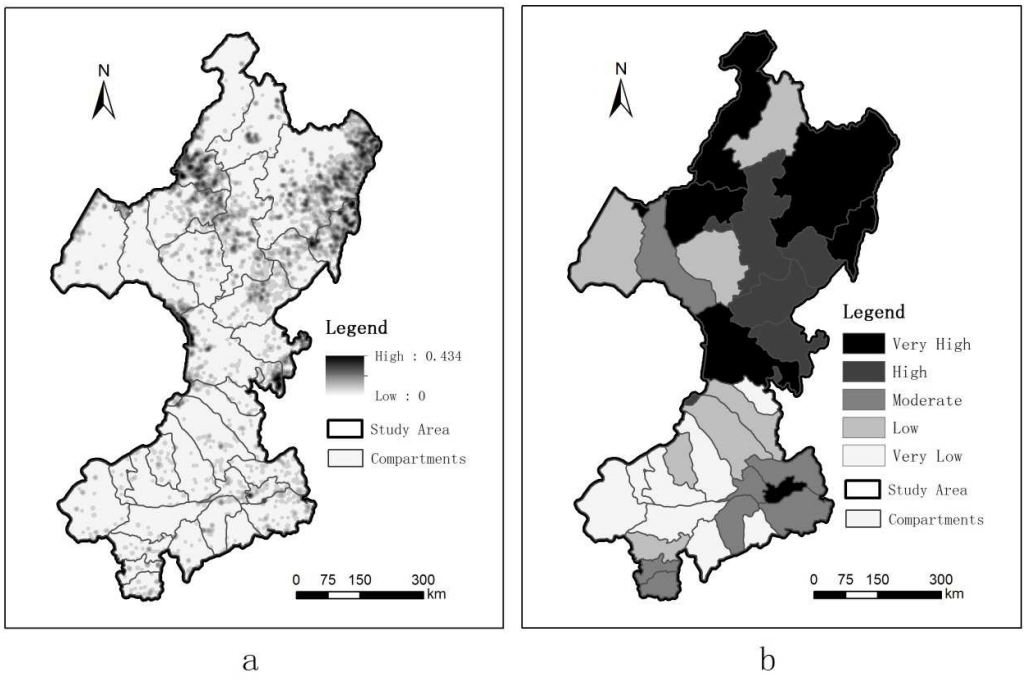

Figure 6: The KDE map of the whole study period (2001-2014) (a) and grassland fire risk map of the study area according to the mean density value of KDE (b)

Associate Editor's Comments to Author:

Associate Editor
Comments to the Author:
The revised version of the manuscript presents a considerable improvement. I still have concerns with the language of the manuscript which, although grammatically correct, frequently reads awkwardly. I would strongly urge the authors to get in touch with a professional language editing service to have native speakers edit the manuscript. I believe the paper warrants publication despite the recommendation for rejection from one of the anonymous reviewers. However, I would recommend a subsequent minor revision following the comments from the reviewers and some very minor comments below:

L19: Imprecise rather than inaccurate positions

A: we accepted it. (Line 19)

L61: Please rephrase "During these events, some fatal accidents can occur, including losses of human lives and economic resources" to something along the lines "These events at times lead to fatal accidents and result in human life loss as well as impose burned of economic resources." It would be nice if you could elaborate what leads to those? Smoke? But if no causes are readily apparent, you could skip it.

A: flame, smoke, heat, etc. can lead to those matters. It cannot be expressed easily. So we deleted this sentence.

Line 202: Please replace "validation" with "accuracy assessment" because validation is a much more rigorous process that requires a lot more precision than using MCD54A1.

A: we accepted it. (Line 203)

Reviewers' Comments to Author:

Reviewer: 1

Comments to the Author
Revisions covered all of my comments. Please update Table 3 with commas in large numbers.

A: Commas was added in the tables. (Line 457)

Reviewer: 2

Comments to the Author
While the authors present interesting work, there is a mismatch between goals and conclusions and the conclusions are not supported by the work. The goals stated are to understand spatial patterns and demonstrate a method. The method is demonstrated, but I do not see any compelling evidence in the manuscript supporting a need for the method within the context presented. The active fire and burned area products used jointly also define spatio-temporal patterns of fire as continuous, areal maps. The conclusions take the goals one step further to say this work produced fire risk zones. Fire risk cannot be determined from past fire events alone and is more accurately described and modeled in Bian et al. 2013 in the Fire Safety Journal.

A: Fire occurrence is due to the comprehensive effect of factors, such as climate, weather, human activities, social economic, fuel mass and moisture. The location of past fire events has higher risk. The neighbors of the past fire events have the similar influencing factors. So the risk of these neighbors is also higher although the fire didn't occur at the locations because fire occurrence has some uncertainty and random. During the period of our study (from 2001 to 2014), the variations of the influencing factors are not very large. So the density derived from the past fire events can express the risk of fire occurrence and the fire risk zone can be used to present the distribution of fire risk.

Fire risk also can be described and modeled by the previous methods. And these methods can not only show the quantitative relationship between the risk and the factors, but also the distribution of fire risk. Even more, the continuous surface of fire density has been proved that they can support the analysis of these models with the corresponding factors.

So, the spatial-temporal patterns of fire distribution can be express by the produced fire risk zones.

In addition, I see some problems with the groupings used for analysis. First, the year ranges given (2001-2005, 2006-2010, 2011-2014) are not three-year periods.

A: the words were changed to "three periods". (Line 210)

Second, the seasonality assessment doesn't make sense since the seasons are defined in the manuscript as quartiles of the annual Julian calendar starting at 1 instead of by climatological indicators.

A: our carelessness led to this mistake. The seasons we used in this study were defined according to climatological indicators (it can be found in the sentences (lines

245-250) compared with table 2). Because the data of MCD45A1 was organized by Julian day, the seasons were compiled according to Julian day too.

In the revised manuscript, the mistake was corrected as follows: spring (Julian day 334-60), summer (Julian day 61-151), autumn (Julian day 152-242) and winter (Julian day 243-333). (Lines 211-212)

While the manuscript has been improved in terms of English language, there still exist some awkward and unclear portions that need additional attention. I strongly encourage editing by a professional service.

A: The manuscript has been improved again by an English speaker. If it need edit again, please notice us.

Finally, please include line numbers in your responses so that reviewers may find your edits more easily.

A: the line numbers were added.